ML-Helio, 23 March, 2022

Resolving the geomagnetic tail current sheet structure with data mining

M. I. Sitnov, G. K. Stephens, H. Arnold, A. Sciola

Johns Hopkins University Applied Physics Laboratory

Linked posters:

G. Stephens+ ”Global Structure of Magnetotail Reconnection Unveiled by Mining Space Magnetometer Data”

H. Arnold+ ”Using Effective Resistivity Maps Derived From Data Mining for Global MHD Simulations of the Magnetosphere”

A. Sciola+ ”Ring Current Plasma Pressure Reconstructed From Empirical Magnetic Field Distributions Embedded within a global MHD model”

Big Data vs. Little Data

An Example of Big Data is New York Stock Exchange that generates about one terabyte of new trade data per day. The statistic shows that 500+terabytes of new data get ingested into the databases of social media site Facebook, every day. /Google, Nov 22, 2021/

Deep learning (Alexnet, 2012): >1 million of 256x256 images (~ 70 billion points)
→processed by ANN (deep CNN) with 4096 nodes → 37,748,736 connections

Earth's magnetosphere

Spaceborne magnetometer data:
~ 10 million points with 5-min cadence over >25 years (since 1995), <~10 points at any moment!

In space we often deal with Little rather than Big Data challenge

3 July 2012 (Angelopoulos et al., 2013)

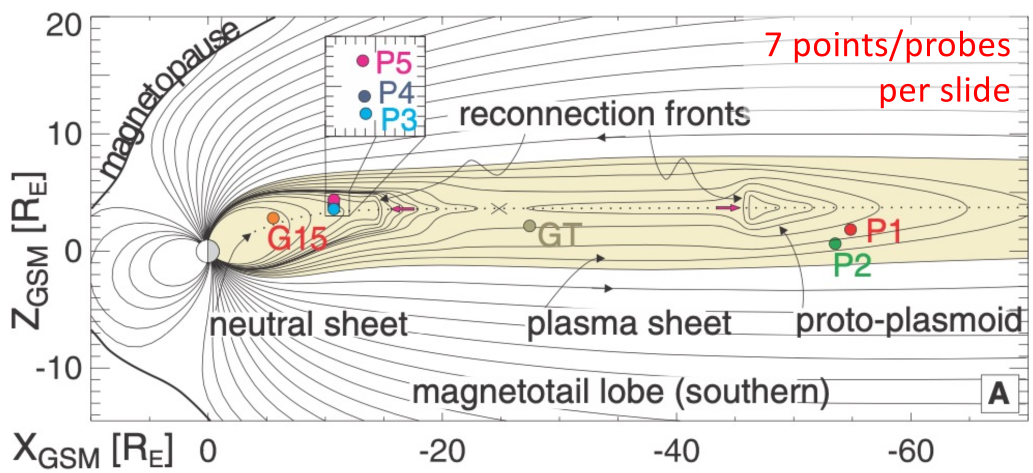

Key to meet the Little Data Challenge: Data Mining (DM) technique

Uses recurring nature of storms and substorms

Mining data in the global parameter space with k_{NN} Nearest Neighbors method (kNN).

K_{NN}~4,000-32,000 virtual probes.

$K_{NN} << K_{Database} \sim 4 \cdot 10^6$

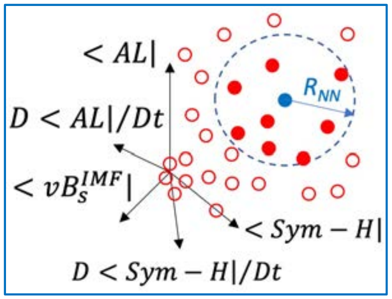

Forming event-oriented subset to fit the magnetic field model (up to 50,000 data points per event)

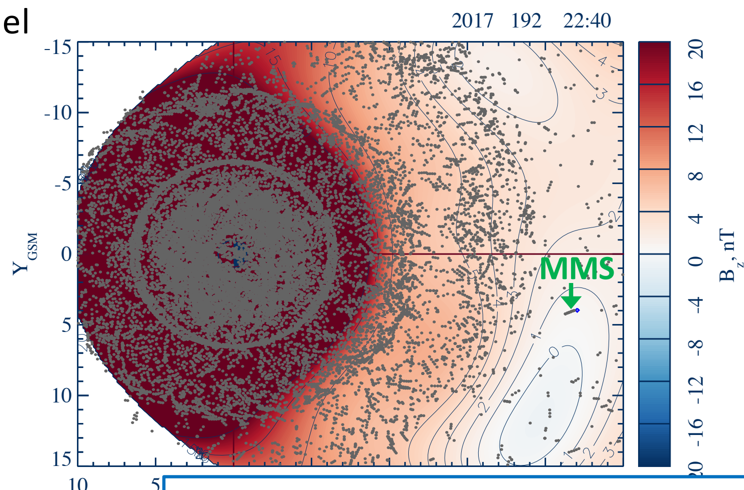

Using sophisticated magnetic field model

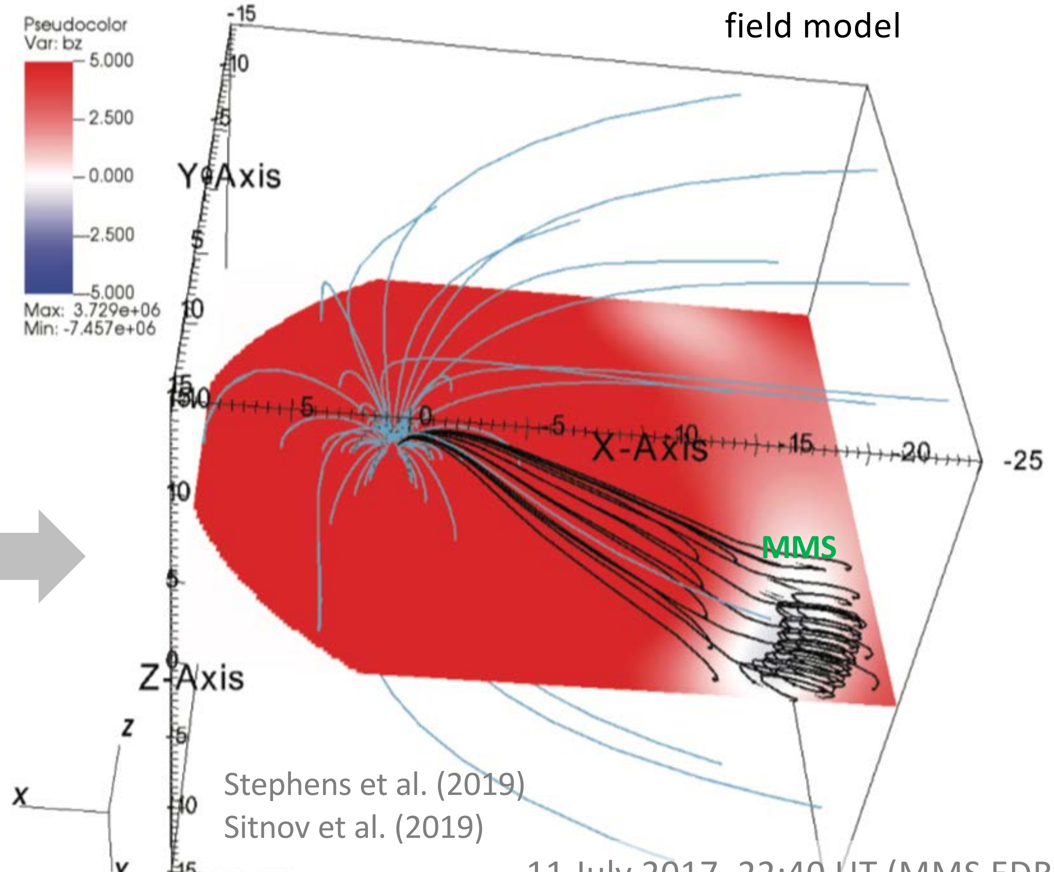

Stephens et al. (2019)
Sitnov et al. (2019)

11 July 2017, 22:40 UT (MMS EDR , Torbert et al., 2018)

kNN DM is an example of lazy (instance–based) learning

kNN DM algorithm

Full set of DM binning parameters

$G_1 = \langle Sym\text{−}H|$ - Captures storm intensity

$G_2 = \dfrac{D\langle Sym\text{−}H|}{Dt}$ - Captures phase of storm

$G_3 = \langle vB_s|$ - Captures substorm loading

$G_4 = \langle AL|$ - Captures substorm intensity

$G_5 = \dfrac{D\langle AL|}{Dt}$ - Captures phase of substorm

$\langle\cdots|$ indicates the data has been smoothed with the following smoothing windows

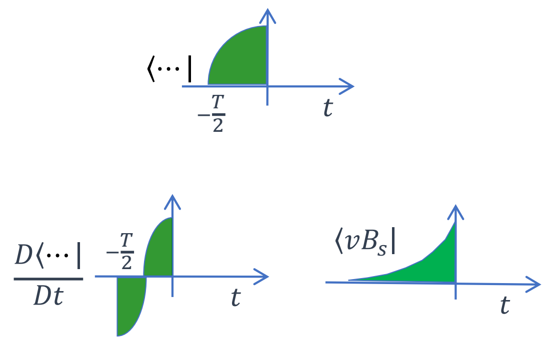

$-\frac{T}{2}$ is taken to be 6 hours (storm scales) for $SymH$ and .5 hours (substorm scales) for AL

$$R_{NN} = \sqrt{\sum_{j=1}^{5} \delta_j G_j^2 / \sigma_{G_j}^2}$$

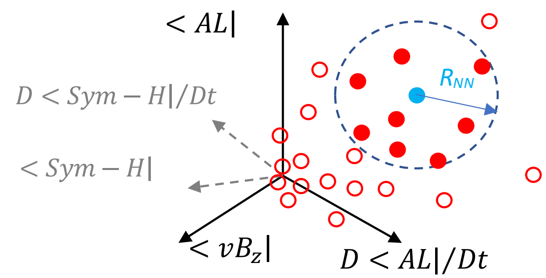

Provides enough probes to avoid overfitting in spatial reconstructions

Provides sensitivity to (sub)storm variations

Key feature:

$$\mathbf{1 \ll K_{NN} \ll K_{DB}}$$

$K_{DB} \approx 4 \cdot 10^6$ points

$K_{NN} = 4 \cdot 10^3 \div 3 \cdot 10^4$

Up to $5 \cdot 10^4$ synthetic probes

Database: >20 probes, >25 years (1995-2020)

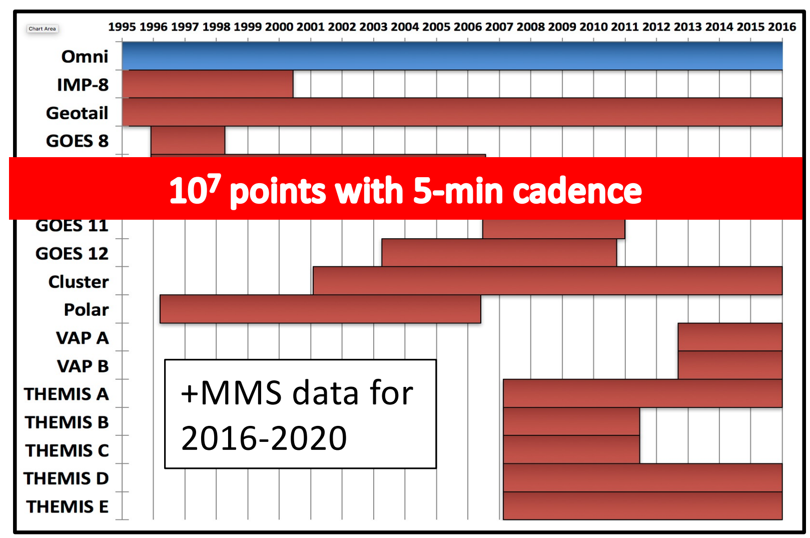

KNN DM algorithm: Data-weighting

Real space weighting

$w_{(0)i} = \Delta N / max(0.2\langle\Delta N\rangle, \Delta N_i)$, $0.5R_E$ bins

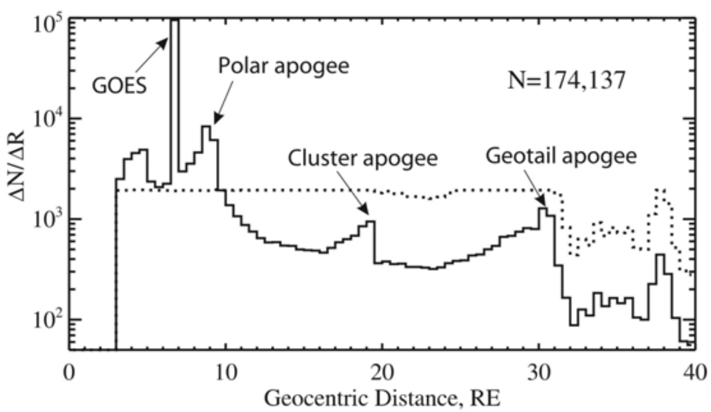

State space weighting

$$M_{err}^{(NN)} = \sqrt{\sum_{j \in S_{NN}} \sum_{i=x,y,z} w_j w_{(0)}(r) \left[B_i^{(mod)}(\mathbf{r}^{(j)}) - B_i^{j,obs}\right]^2}$$

$$w_j = \exp\left[-\left(R_q^{(j)}/\sigma R_{NN}\right)^2/2\right]$$

KNN bin in the real space

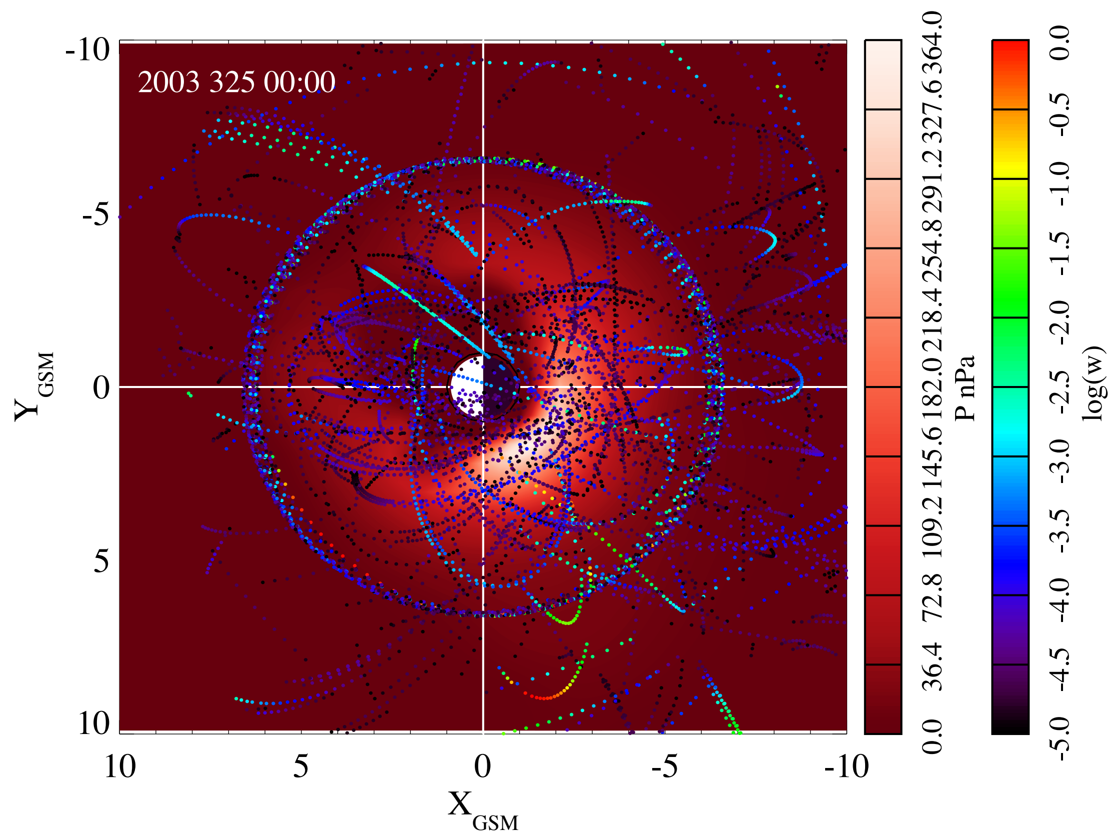

Color-coded is the proximity to the query point in the global parameter space

Key elements of magnetic field architecture

Equatorial currents

$$\mathbf{B}_E = \mathbf{B}_{CF} + \underbrace{\mathbf{B}_T + \mathbf{B}_{SRC} + \mathbf{B}_{PRC}} + \mathbf{B}_{FAC} + \mathbf{B}_{INT}$$

$$\boxed{\mathbf{B}_T = \sum_{n=1}^{N} t_n^{(s)} \mathbf{B}_{Tn}^{(s)} + \sum_{m=1}^{M}\sum_{n=1}^{N} t_{mn}^{(o)} \mathbf{B}_{Tmn}^{(o)} + \sum_{m=1}^{M}\sum_{n=1}^{N} t_{mn}^{(e)} \mathbf{B}_{Tmn}^{(e)}}$$

$$t = t^{(0)} + t^{(1)} \sqrt{P_d},$$

Basic idea: Magnetic field of axisymmetric current disc (*Tsyganenko*, 1989)

Ampere's equation
$$\frac{\partial}{\partial \rho}\left(\frac{1}{\rho}\frac{\partial}{\partial \rho}\left(\rho A_\phi\right)\right) + \frac{\partial^2 A_\phi}{\partial z^2} = J_\phi(\rho)\delta(z)$$

Solution
$$A_\phi(\rho, z) = \int_0^\infty C(k)\exp\left(-k|z|\right)J_1(k\rho)\sqrt{k}\,dk$$

Finite sum form:
$$A_\phi(\rho, z) = \sum_{n=0}^{N} C_n e^{-k_n|z|} J_1(k_n\rho) \qquad k_n = \frac{n}{\rho_0}$$

$$|z| \rightarrow Z = \sqrt{z^2 + D^2}$$

Sample basis function:

$$\mathbf{B}_{Tmn}^{(o)} = k_n J_m(k_n\rho)\exp(-$$

Field-aligned currents

Basic element (Tsyganenko, 2002)

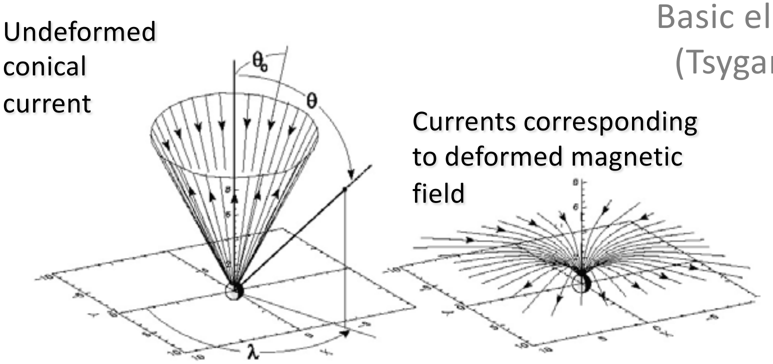

Coupling with equatorial currents

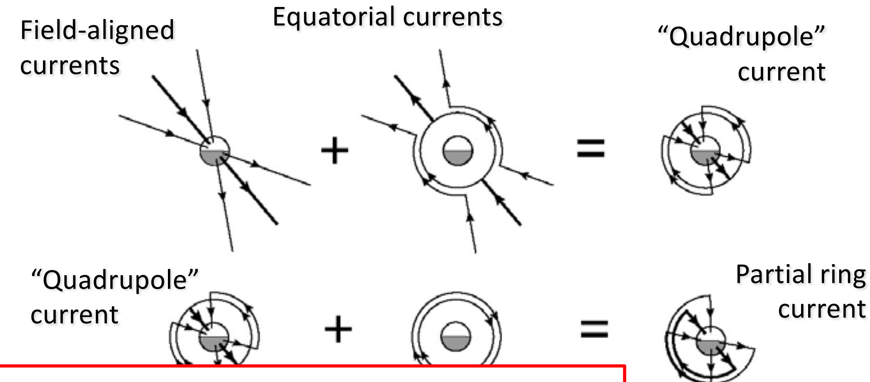

and azimuthal angle

We use lots of Tsyganenko's math (because it is often physics-based) but get rid of Tsyganenko's original concepts of custom tailored statistical models of the geomagnetic field

Key elements of magnetic field architecture: Substorm features

Using two independent current sheet expansions to capture inhomogeneous CS thinning and the formation of embedded and bifurcated thin current sheets (TCSs).

$$B^{(eq)}_{(s-s)} = B^{(eq)}\left(\rho,\phi;D\right) + B^{(eq)}_{TCS}\left(\rho,\phi;D_{TCS}\right)$$

$$\boxed{D_{TCS} < D_0 \sim 1R_E}$$

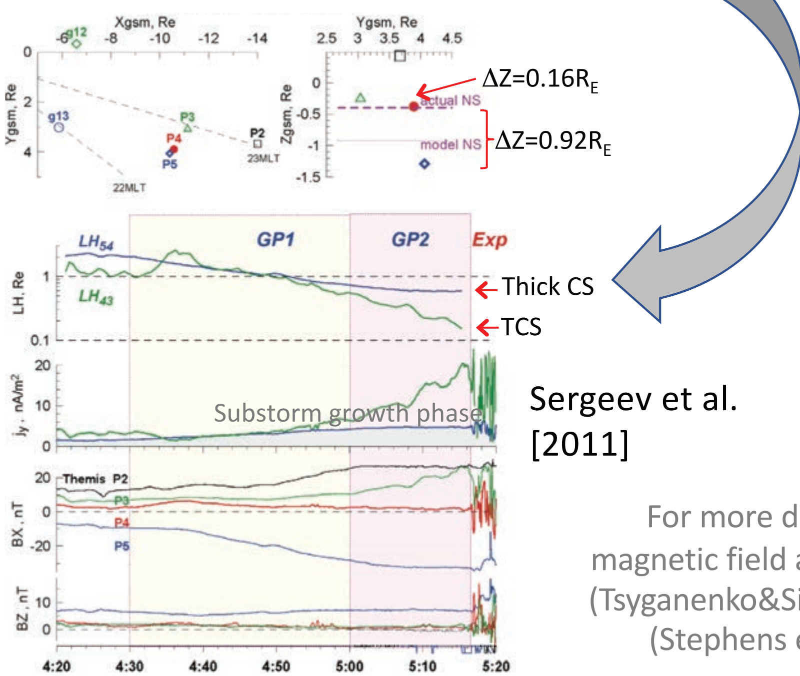

Sergeev et al. [2011]

Flexible system of the field-aligned currents (FAC)

- Rigid FAC modules are replaced by an expansion of modules shifted in latitude

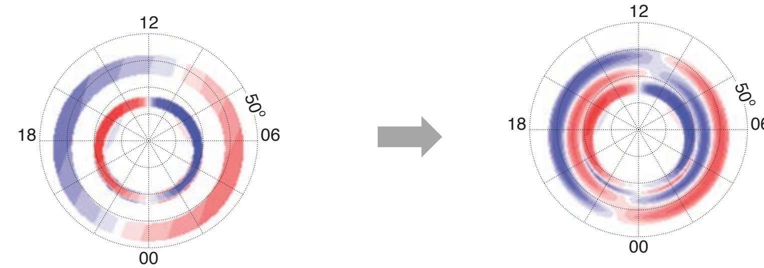

- Allows the FAC structure to more closely match low-altitude data

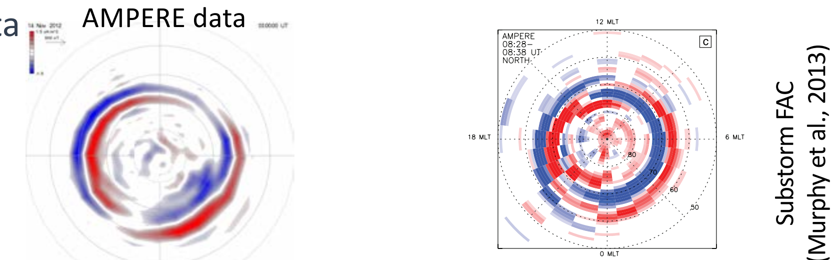

- And the Harang discontinuity

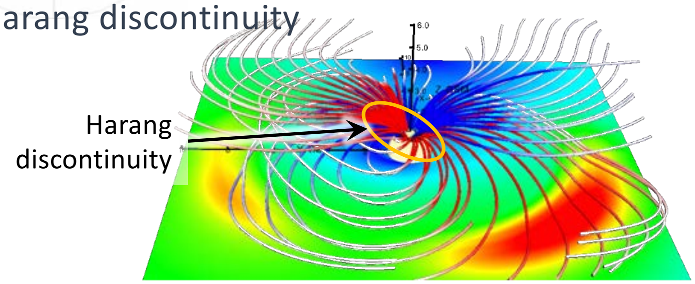

For more details of the magnetic field architecture see (Tsyganenko&Sitnov, 2007) and (Stephens et al., 2019)

Validation and uncertainty quantification

Validation

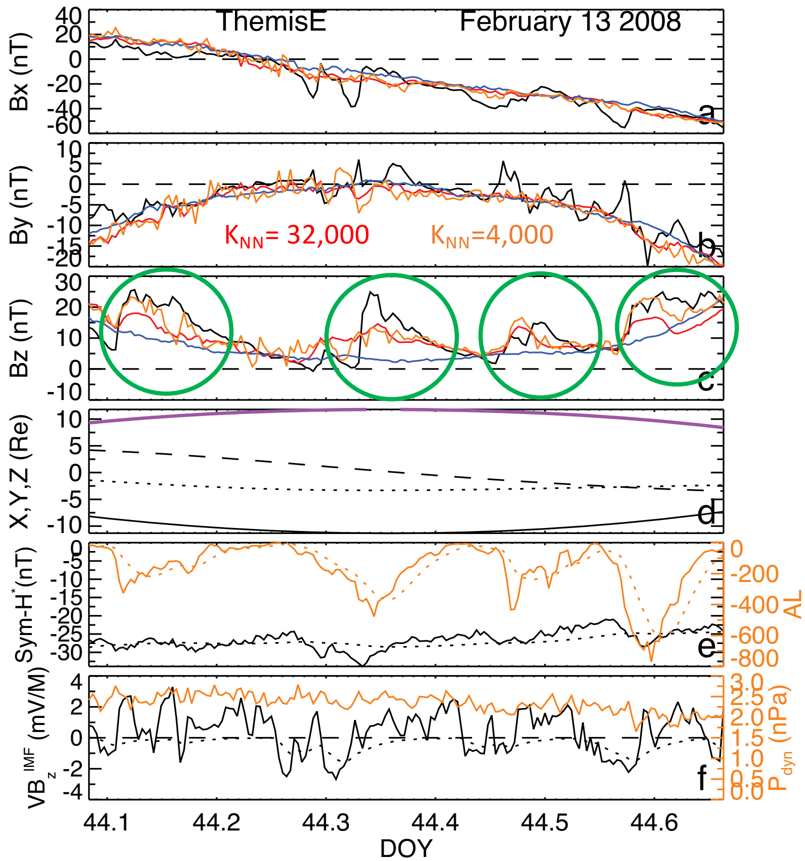

Red lines – averages of binning parameters over their KNN subsets with K_{NN}=32,000. Blue lines are the corresponding standard deviations.

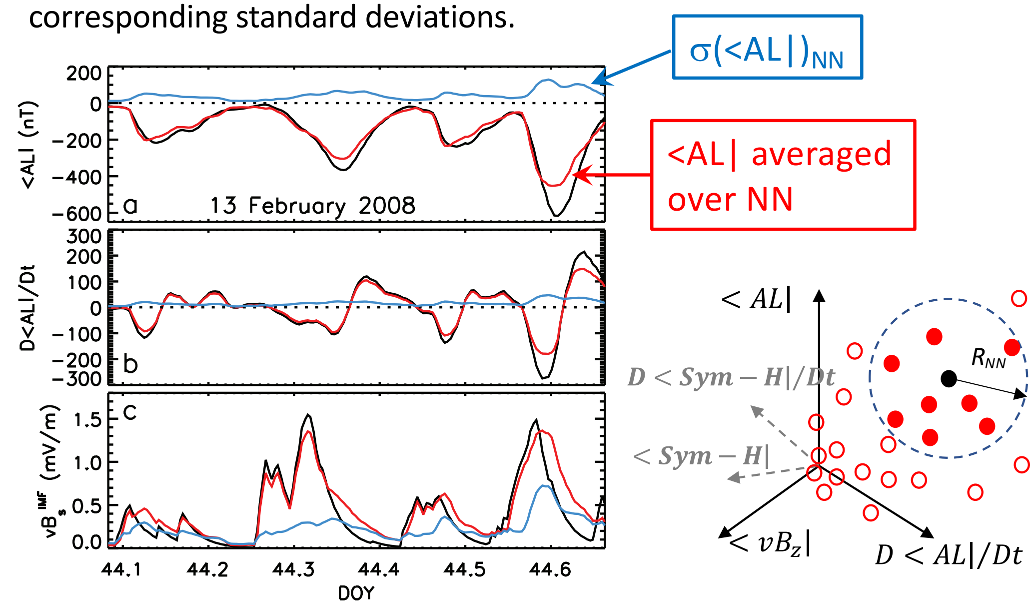

Statistical uncertainty in DM subsets (equivalent to 10^4 THEMIS missions!) is much smaller compared to major variations of the key parameter means. Systematic biases are small.

KNN DM is most interesting as a Data Discovery (DD) tool

DD1: Buildup and decay of TCS in 13 February 2008 substorms

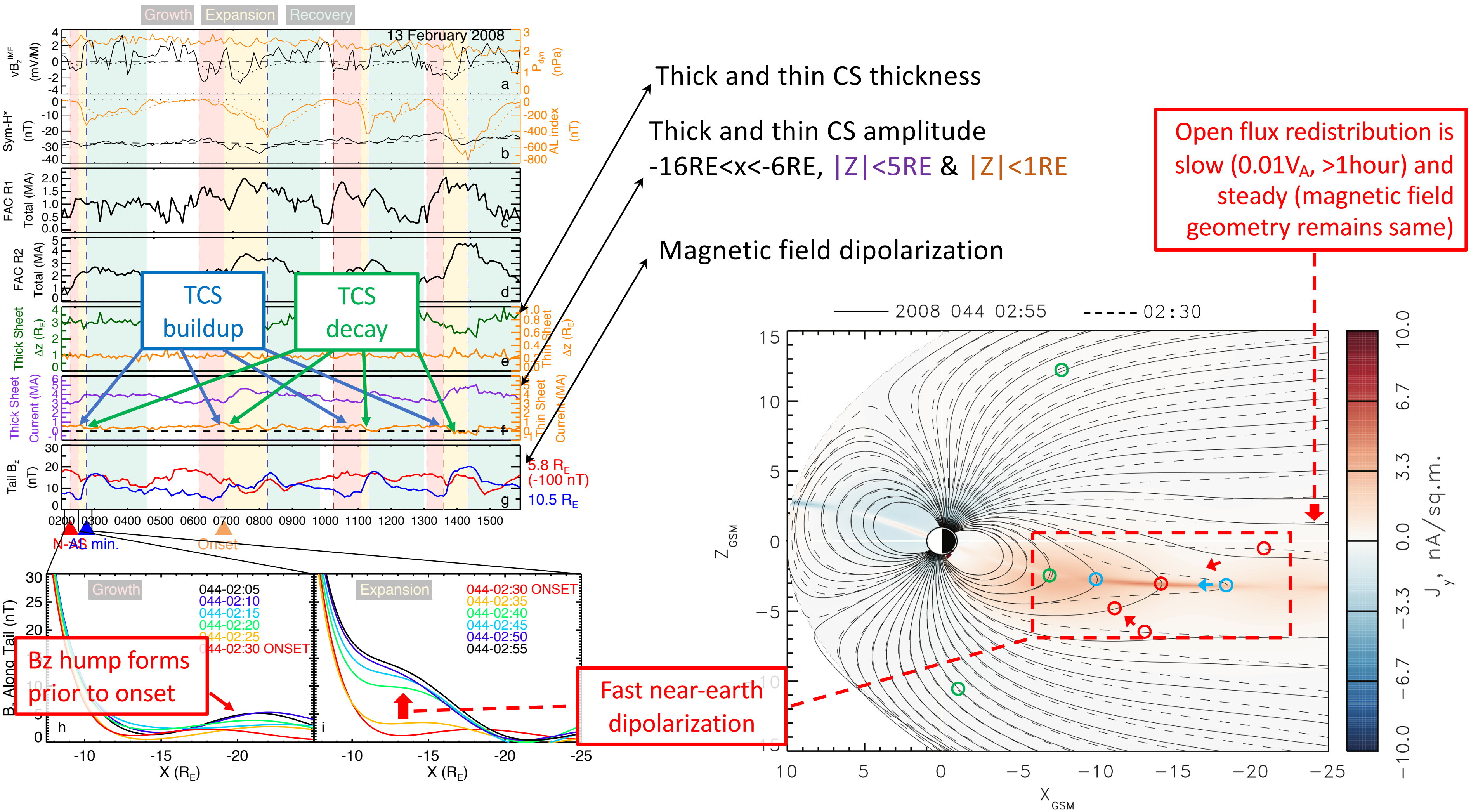

February 13, 2008 event#1: Spatial distributions of the magnetic field and electric current

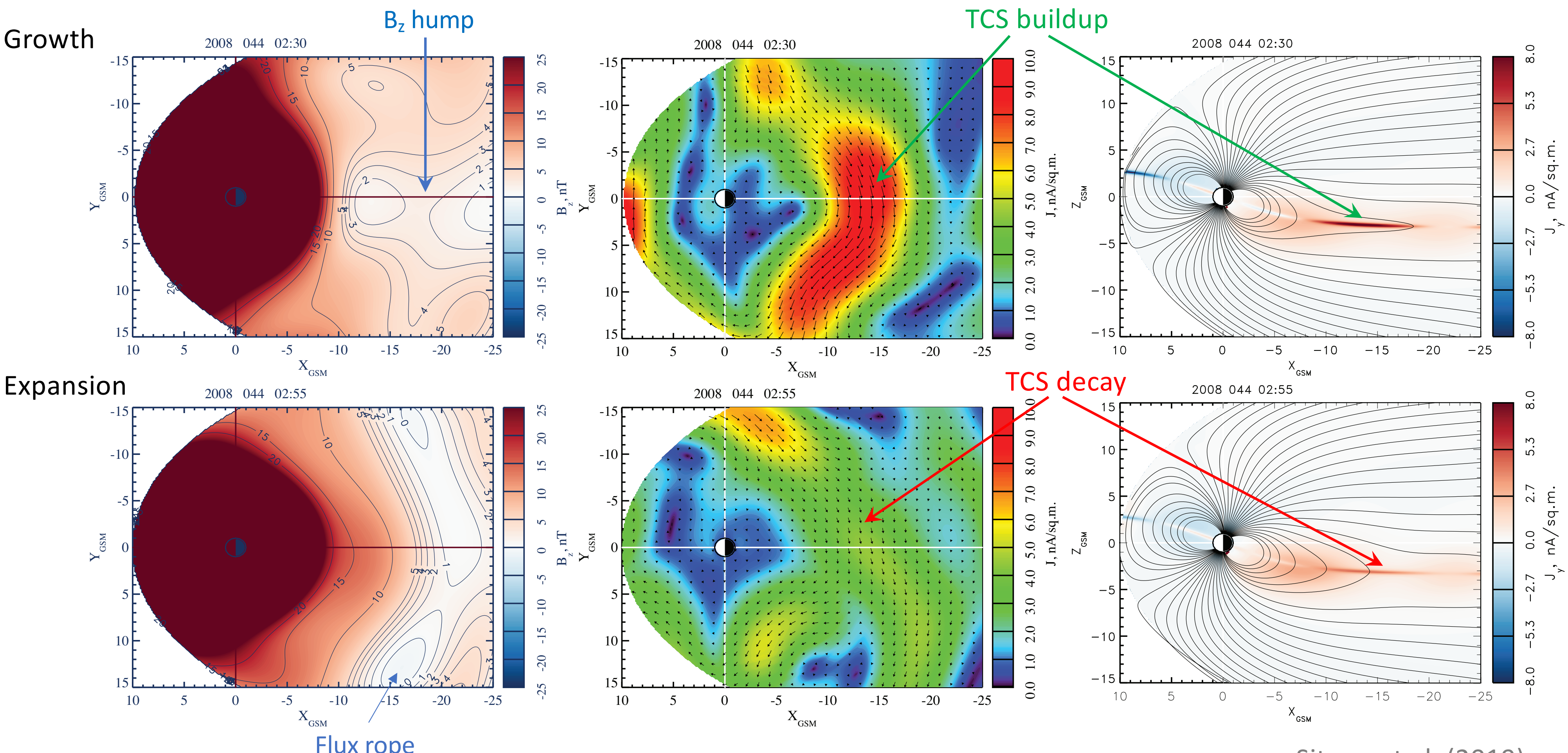

Sitnov et al. (2019)

DD2: Isotropic force balance violation and TCS scaling

February 13, 2008 substorm

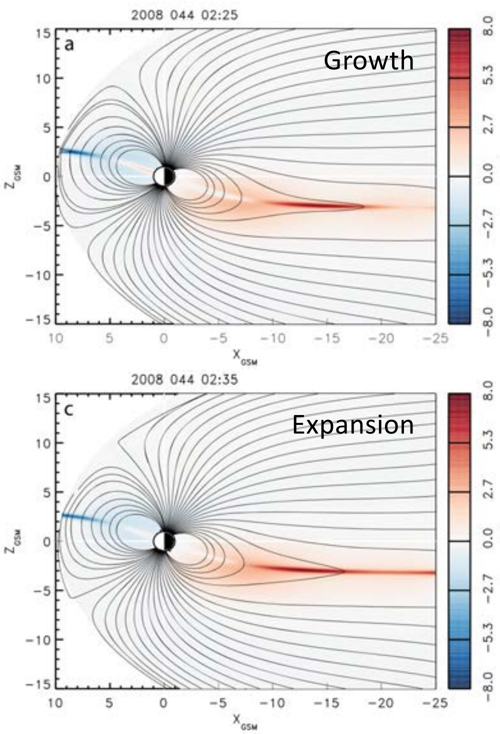

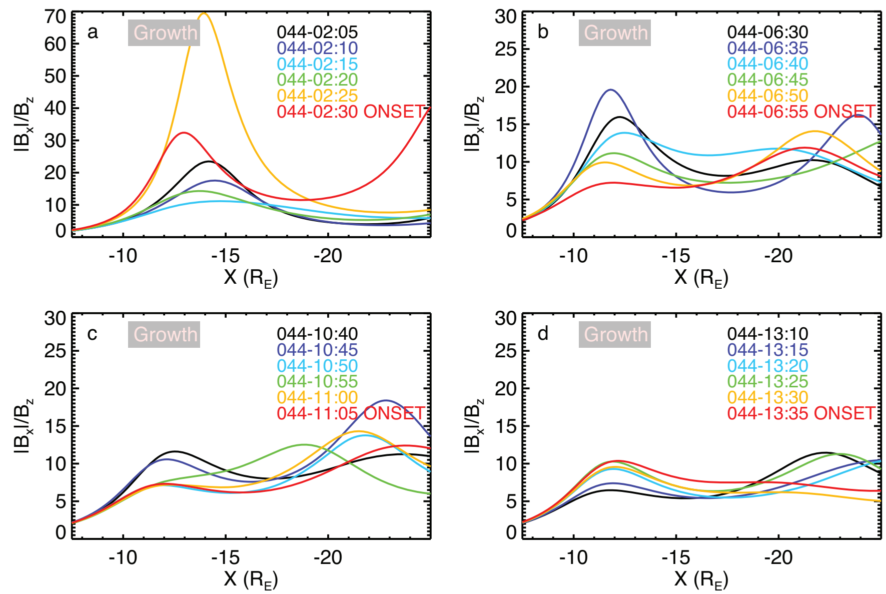

$B_0/B_z \sim 10$

Violates isotropic force balance: $L_x/L_z \sim B_0/B_z$ (Cole and Schindler, 1972; Rich et al., 1972)

TCS aspect ratio ($L_z \sim 0.2R_E$): $L_x/L_z \sim 75$ → $(L_x/L_z)/(B_0/B_z) \sim 7.5$

In the substorm growth phase the isotropic force balance is violated and it requires to go beyond isotropic plasma models (including MHD)

Key elements of magnetic field architecture: Further TCS adjustment I

Harris model

$f_{0\alpha} \propto exp[-(W_\alpha - v_{D\alpha}P_{y\alpha})/T_\alpha]$,
$\alpha = e, i$

Neutrality condition: $\frac{v_{Di}}{v_{De}} = -\frac{T_i}{T_e}$

Integrals of motion: $W_\alpha = m_\alpha v^2/2 + q_\alpha \phi$

$P_\alpha = m_\alpha v_y + (q_\alpha/c)A_y$

Dimensionless parameters and variables:
$\tau = T_e/T_i, w_{D\alpha} = v_{D\alpha}/v_{T\alpha}, \zeta = z/\rho_{0i},$

$\beta_0 = 8\pi n_0 T_i/B_0^2, b = B_x/B_0,$
$a = -A_y/(B_0\rho_{0i})$

Solution:

$a(\zeta) = \log(\cosh(\zeta w_{Di}))/w_{Di}$,

$b(\zeta) = \tanh(\zeta w_{Di})$,

$n(\zeta) = n_0/(\cosh(\zeta w_{Di}))^2$,

Isotropic force balance:

$$\frac{\partial p}{\partial x} = J_y B_z$$

$$\frac{B_x^2}{L_x} \sim \frac{B_x}{L_z} B_z$$

Empirical reconstruction of thin current sheets

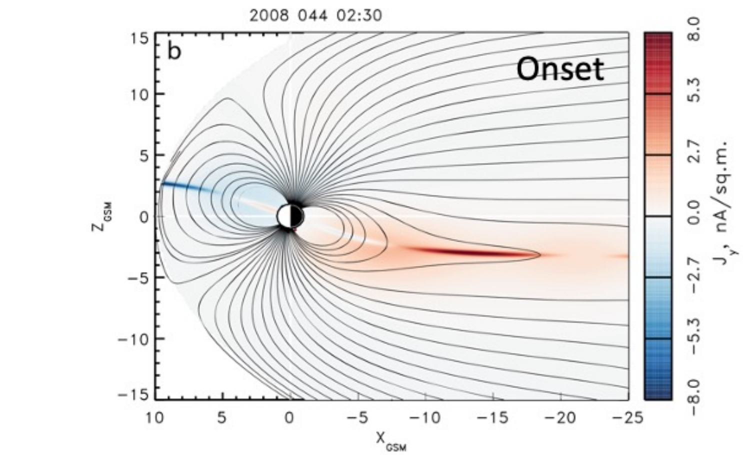

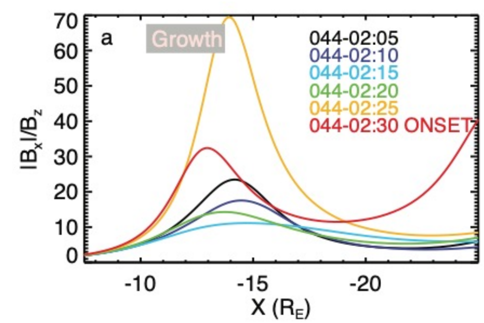

$$\frac{L_x}{L_z}\frac{B_z}{B_0} \gg 1$$

Thin ion-scale current sheets violate the isotropic force balance in the tail $\frac{\partial p}{\partial x} = J_y B_z$

Key elements of magnetic field architecture: Further TCS adjustment I

Tail plasma is weakly anisotropic

Artemyev et al. (2019)

Weak field-aligned ion anisotropy

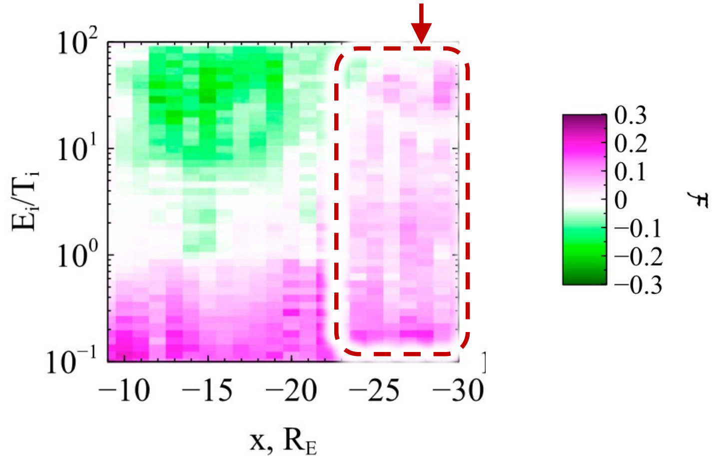

$$\mathcal{F} = (F_{\parallel} - F_{\perp})/(F_{\parallel} + F_{\perp}),$$

$F_{||}$ is ion fluxes averaged over pitch angle ranges of [0, 30°], [150° , 180°] and $F_{\perp}$ is ion fluxes averaged over pitch angle ranges of [75°, 105°].

Non-Harris TCS model

Sitnov, Guzdar, Swisdak (2003)

$$f_{0\alpha} \propto \exp\left(-\frac{2W_\alpha - \omega_{0\alpha} I_z^{(\alpha)}}{2T_{\|\alpha}} + \frac{v_{D\alpha} P_{y\alpha}}{T_{\|\alpha}} - \frac{\omega_{0\alpha} I_z^{(\alpha)}}{2T_{\perp\alpha}}\right)$$

Quasi-adiabatic invariant: $I_z^{(\alpha)} = \frac{1}{2\pi} \oint m_\alpha v_z dz$

Velocity shear

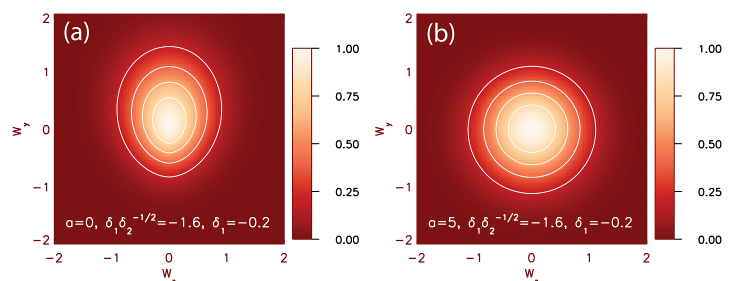

$$b(\zeta) = \frac{\zeta}{|\zeta|} \sqrt{(\tanh w_{Di}\zeta_1(\zeta))^2 + \frac{4|\delta_1| b^{(tcs)}(a_0(\zeta))}{\pi^2(1+\tau)(2w_{Di})^{1/2}}} \Big/ \sqrt{1 + \frac{4|\delta_1| b_{(\infty)}^{(tcs)}}{\pi^2(1+\tau)(2w_{Di})^{1/2}}},$$

$\delta_1 = T_{\perp i}/T_{||i} - 1,$
$|\delta| \ll 1,$
$\delta_2 = v_{Di}/v_{\perp Ti} \ll 1$

(Zenitani and Nagai, 2016)

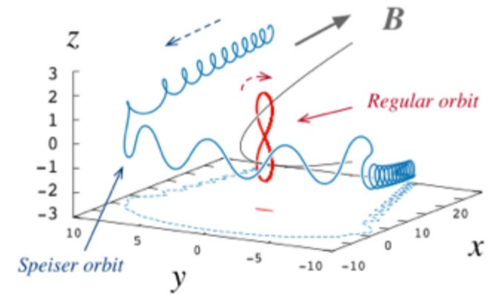

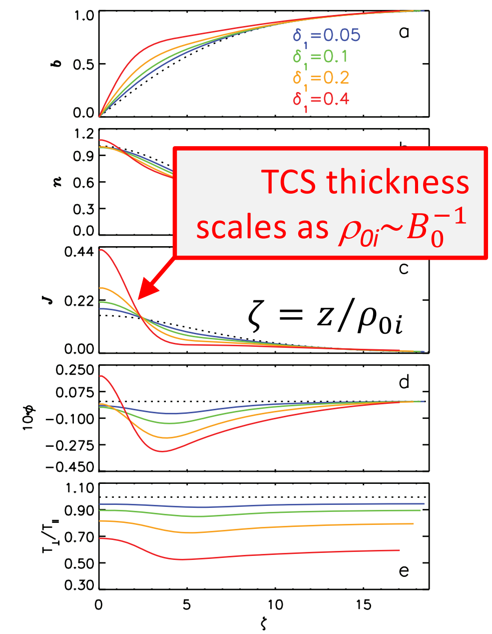

Key elements of magnetic field architecture: Further TCS adjustment III

Lobe field variation along the tail (Wang et al., 2004)

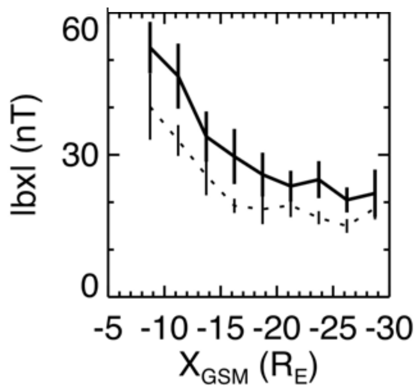

Advanced TCS approximation:

$$D_{TCS}(x,y) = \left(\alpha e^{-\beta\rho'} + D_0^{-1}\right)^{-1}$$

$$\rho' = \sqrt{(x-x_0)^2 + y^2}$$

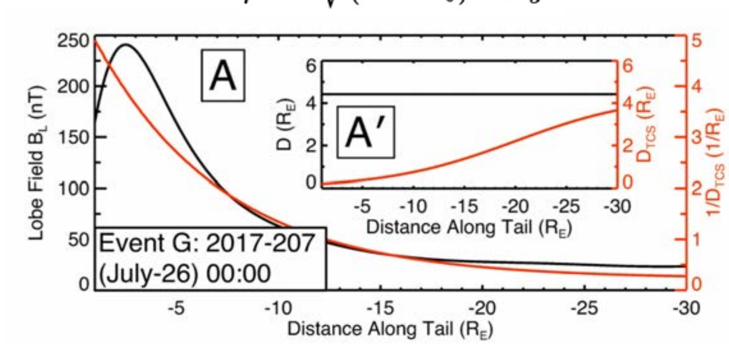

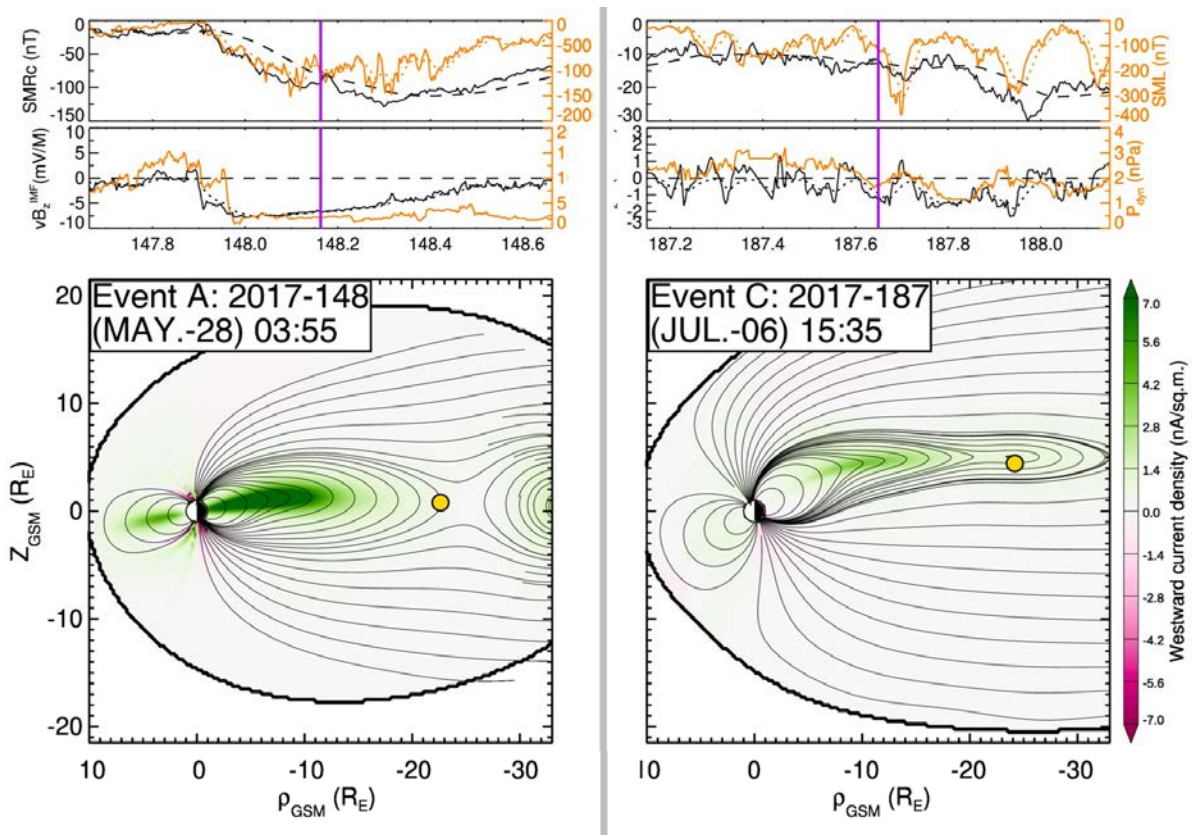

Global structure of the multi-scale magnetotail current sheet

Summary

- Mining sparse spaceborne magnetometer data becomes possible due to the recurrent nature of storms and substorms. Moreover, it is incredibly successful: One can reconstruct almost all detected X-lines, thin embedded TCS with Speiser orbits and even the storm time ring current and plasma pressure.

- But it requires special techniques, such as distance-weighted kNN and flexible physics-based geomagnetic field architectures.

- Data mining suggests that the buildup and decay of thin ion-scale current sheets is one of the most characteristic features of magnetospheric substorms.